

# Dynamics of Dark-Bright Solitons in Cigar-Shaped Bose-Einstein Condensates

S. Middelkamp,<sup>1</sup> J.J. Chang,<sup>2</sup> C. Hamner,<sup>2</sup> R. Carretero-González,<sup>3</sup> P. G. Kevrekidis,<sup>4</sup> V. Achilleos,<sup>5</sup> D.J. Frantzeskakis,<sup>5</sup> P. Schmelcher,<sup>1</sup> and P. Engels<sup>2</sup>

<sup>1</sup>Zentrum für Optische Quantentechnologien, Universität Hamburg, 22761 Hamburg, Germany

<sup>2</sup>Washington State University, Department of Physics & Astronomy, Pullman, WA 99164 USA

<sup>3</sup>Nonlinear Physics Group, Departamento de Física Aplicada I, Universidad de Sevilla, 41012 Sevilla, Spain

<sup>4</sup>Department of Mathematics and Statistics, University of Massachusetts, Amherst MA 01003-4515, USA

<sup>5</sup>Department of Physics, University of Athens, Panepistimiopolis, Zografos, Athens 157 84, Greece

We explore the stability and dynamics of dark-bright solitons in two-component elongated Bose-Einstein condensates by developing effective 1D vector equations as well as solving the corresponding 3D Gross-Pitaevskii equations. A strong dependence of the oscillation frequency and of the stability of the dark-bright (DB) soliton on the atom number of its components is found. Spontaneous symmetry breaking leads to oscillatory dynamics in the transverse degrees of freedom for a large occupation of the component supporting the dark soliton. Moreover, the interactions of two DB solitons are investigated with special emphasis on the importance of their relative phases. Experimental results showcasing dark-bright soliton dynamics and collisions in a BEC consisting of two hyperfine states of <sup>87</sup>Rb confined in an elongated optical dipole trap are presented.

*Introduction.* Multi-component systems of nonlinear waves are a fascinating topic with a rich and diverse history spanning a variety of areas, including Bose-Einstein condensates (BECs) in atomic physics [1], optical fibers and crystals in nonlinear optics [2], and integrable systems in mathematical physics [3]. Of particular interest are the so-called “symbiotic solitons”, namely structures that would not otherwise exist in one-component settings, but can be supported by the interaction between the optical or atomic species components. A prototypical example of such a structure is the dark-bright (DB) soliton in self-defocusing, two-component systems, whereby the dark soliton (density dip) which typically arises in self-defocusing media [1–4] creates, through nonlinearity, a trapping mechanism that localizes a density hump (bright soliton) in the second component.

Dark-bright solitons were experimentally created in photorefractive crystals [5], while their interactions were partially monitored in [6]. Upon realization of multi-component atomic BECs [7–9], it was predicted that similar structures would exist therein [10]. While theoretical developments along this direction were extended in even more complex settings (such as the spinor system of Ref. [11]), *stable* DB solitons were observed only recently in two-component BECs [12], leading to a renewed interest in this area. Relevant recent works include the interaction between DB solitons [13, 14] and their higher-dimensional generalizations [15].

In order to study DB solitons in two-component elongated BECs we will use both effectively one-dimensional (1D) mean-field models and the full 3D Gross-Pitaevskii equation (GPE). For a single species, quasi-1D descriptions rely on the non-polynomial Schrödinger equation (NPSE) [16] and the Gerbier-Muñoz-Mateo-Delgado equation (GMDE) [17]; these models have been used in studies of dark solitons in the dimensionality crossover

between 1D and 3D, yielding excellent quantitative agreement with experimental observations [18]. However, in multi-component settings only the NPSE equation has been derived [19]. In the present work, we first develop the GMDE for two-component BECs and then investigate the DB soliton statics and dynamics using the NPSE, the GMDE and the 3D GPE. Varying the atom number of either the dark ( $N_D$ ) or the bright ( $N_B$ ) component, we find that in a harmonic trap *the soliton oscillation period may change by nearly one order of magnitude*; most notably, the bright component is shown to slow down the oscillation of the dark one. Our investigation reveals a feature absent in the dark soliton dynamics in one-component BECs, namely that *a single DB soliton may become dynamically unstable*. Increasing  $N_D$  and  $N_B$  reveals a deviation from the effective 1D description: specifically, *an increase of  $N_D$  leads to a spontaneous breaking of the cylindrical symmetry*, manifested in a transversal oscillation of the bright component, and a subsequent decrease of the axial DB oscillation frequency. Moreover, we analyze the interaction between multi-DB solitons and the role of their relative phase. Our results pertain to the hyperfine states  $|1, -1\rangle$  and  $|2, 0\rangle$  of <sup>87</sup>Rb, as in the experiment of Ref. [12], and also for the states  $|1, -1\rangle$  and  $|2, -2\rangle$  of <sup>87</sup>Rb in an optical dipole trap. For the latter states, *we present experimental results concerning the DB soliton oscillations and multi-DB soliton interactions* that further support our findings.

*Effective 1D Theory.* The macroscopic wave functions of Bose condensed atoms in two different internal states obey the following vector GPEs [1]:

$$i\hbar \frac{\partial \psi_k}{\partial t} = \left( -\frac{\hbar^2 \nabla^2}{2M} + U + g_{kk} |\psi_k|^2 + g_{12} |\psi_{3-k}|^2 \right) \psi_k, \quad (1)$$

where  $\psi_k(\mathbf{r})$  are the macroscopic wave functions ( $k = 1, 2$ ), normalized to  $N_D$  and  $N_B$  for the dark and bright soliton components, respectively,  $g_{ij} = 4\pi \hbar^2 a_{ij}/M$  are

the effective nonlinear coefficients due to the  $s$ -wave scattering for  $i, j = 1, 2$ , and  $U(\mathbf{r})$  is the confining potential. For a highly anisotropic trap, we first factorize the wave function as  $\psi_k(\mathbf{r}, t) = \phi_k(\mathbf{r}_\perp; x)f_k(x, t)$  [16, 17], we substitute in Eq. (1), multiply by  $\phi_k^*(\mathbf{r}_\perp; x)$  and, finally, integrate over the transverse directions; this leads to the following effective 1D model:

$$\left[ i\hbar \frac{\partial}{\partial t} + \frac{\hbar^2}{2M} \frac{\partial^2}{\partial x^2} - V(x) \right] f_k = \mu_{\perp k} [f_k] f_k, \quad (2)$$

where  $V(x) = M\omega_x^2 x^2/2$  is the axial potential and the transverse chemical potential  $\mu_{\perp k} = \mu_{\perp k}[f_k(x, t)]$  is a functional of  $f_k$ :

$$\begin{aligned} \mu_{\perp k}[f_k] = & \int d^2\mathbf{r}_\perp \phi_k^* \left( -\frac{\hbar^2}{2M} \nabla_\perp^2 + \frac{1}{2} M \omega_\perp^2 r_\perp^2 \right. \\ & \left. + g_{kk} |\phi_k|^2 |f_k|^2 + g_{12} |\phi_{3-k}|^2 |f_{3-k}|^2 \right) \phi_k, \quad (3) \end{aligned}$$

where  $(\omega_x, \omega_\perp)$  are the trap frequencies along the longitudinal (axial) and transverse directions, and we have assumed that the derivatives of  $\phi_k$  do not depend on the axial variable  $x$ . For an effectively 1D system, we assume that the transverse wave function remains in its Gaussian ground-state,  $\phi_k = \frac{1}{\pi\sqrt{\sigma_k}} \exp(-\frac{r_\perp^2}{2\sigma_k^2})$ . To account for axial effects, we allow the width  $\sigma_k$  to be a variational parameter,  $\sigma_k = \sigma_k[f_k(x, t)]$ ; this yields:

$$\mu_{\perp k} = \frac{\hbar^2}{2M} \sigma_k^{-2} + \frac{M}{2} \omega_\perp^2 \sigma_k^2 + \frac{g_{kk} |f_k|^2}{2\pi} \sigma_k^{-2} + \frac{g_{12} |f_{3-k}|^2}{\pi(\sigma_1^2 + \sigma_2^2)}.$$

There are two different approaches to determine  $\sigma_k$ : one can minimize the chemical potential  $\mu_{\perp k}$  with respect to  $\sigma_k$  for given  $f_k(x, t)$  or, alternatively, one can use the Euler-Lagrange equations from the Lagrangian associated to Eq. (2), minimizing the total energy [19]. These two approaches lead to the following expression for  $\sigma_k$ ,

$$\sigma_k^4 = \frac{\hbar^2}{\omega_\perp^2 M^2} + \frac{g_{kk} |f_k|^2}{A\pi M \omega_\perp^2} + \frac{2g_{12} |f_{3-k}|^2}{\pi M \omega_\perp^2 (\sigma_1^2 + \sigma_2^2)^2} \sigma_k^4, \quad (4)$$

where parameter  $A = 1$  corresponds to the GMDE system and  $A = 2$  for the NPSE system. Notice that Eqs. (2) and (4) constitute a set of coupled nonlinear equations which have to be solved consistently in order to obtain  $f_k(x, t)$  and  $\sigma_k[f_k(x, t)]$ .

Using the above approach, we will investigate the trapped dynamics of a DB soliton in a quasi-1D condensate. For the 1D case without a trap in the axial direction ( $V(x) = 0$ ), and assuming that all scattering lengths are equal, there exists an analytical DB soliton solution of Eqs. (1) [10]; this can be expressed in the following dimensionless form (in units so that  $\hbar = M = 1$ ),

$$\psi_D = \nu \sqrt{\mu} \sin \alpha + \sqrt{\mu} \cos \alpha \tanh(\kappa(x - q(t))), \quad (5)$$

$$\psi_B = \sqrt{\frac{N_B \kappa}{2}} e^{i(\phi + \omega_B t + x \kappa \tan \alpha)} \operatorname{sech}(\kappa(x - q(t))). \quad (6)$$

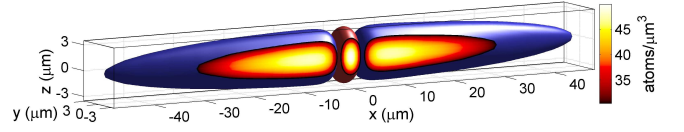


FIG. 1: (Color online) Iso-level contours at 2/5 of the maximal density (dark/bright soliton depicted in blue/red) of a DB soliton as a result of 3D GPE simulations ( $N_D = 93\,367$ ,  $N_B = 7\,926$ ). The transverse cut ( $y = \text{const.}$ ) shows the atom density with the scale depicted by the colorbar.

Here,  $\psi_D$  is the dark soliton (on top of a constant background with chemical potential  $\mu = \mu_D$ ), with an inverse width  $\kappa = \sqrt{\mu \cos^2 \alpha + (N_B/4)^2} - N_B/4$ , position  $q(t) = q(0) + t\kappa \tan \alpha$  and phase angle  $\alpha$ , whereas  $\psi_B$  is the bright soliton that is symbiotically supported by the dark one with the same width and position. In the realistic case of the hyperfine states  $|1, -1\rangle$  and  $|2, 0\rangle$  of  $^{87}\text{Rb}$ , the scattering lengths are different ( $a_{11} = 100.86a_0$ ,  $a_{22} = 94.57a_0$  and  $a_{12} = 98.98a_0$ ). Nevertheless, in the quasi-1D setting (with the trap), we have found that there exists a stationary DB state [cf. Eqs. (5)-(6) with  $\alpha = 0$ ] located at the trap center. We identify this state,  $f_k^{\text{stat}}$ , using a fixed-point algorithm, and then perform a Bogoliubov-de-Gennes (BdG) analysis to determine its linear stability by using the ansatz  $f_k = f_k^{\text{stat}} + (u_k(x) \exp(i\omega t) + v_k^*(x) \exp(-i\omega^* t))$ . The eigenfrequencies  $\omega$  and amplitudes  $(u_k, v_k)$  of the ensuing BdG linearization operator encode the dynamical stability of the system: for vanishing imaginary part  $\omega_i$  of  $\omega = \omega_r + i\omega_i$ , the system is dynamically stable and  $\omega_i \neq 0$  implies dynamical instability. We also note that the eigenfrequency of the anomalous (negative energy) mode of the spectrum (see below) coincides with the oscillation frequency of the DB soliton, similarly to dark solitons in one-species BECs [18].

*Results.* We have chosen a cylindrical trap with frequencies  $\omega_\perp = 2\pi \times 133$  Hz and  $\omega_x = 2\pi \times 5.9$  Hz, similar to the ones used in the experiment of Ref. [12]. In Fig. 1 we show iso-level contours of a DB soliton resulting from numerical integration of the 3D GPE, while in Fig. 2 we compare the oscillation period (frequency) derived by the effective 1D model against results of the 3D GPE. The top panel illustrates the dependence of the period of the DB soliton on the number of atoms ( $N_D, N_B$ ) of the two components. It is clear that variation of the number of atoms, especially in the bright component by a factor of 2, may lead to a significant (approximately two-fold) variation of the DB soliton frequency. The agreement between 1D and 3D generally becomes worse when  $N_B$  is increased and, to a lesser extent, when  $N_D$  is increased. Notice that the NPSE model yields generally more accurate predictions than the GMDE one.

The bottom panels of Fig. 2 show the DB soliton spectrum. When the anomalous mode collides with a mode of positive energy, the DB soliton becomes dynamically

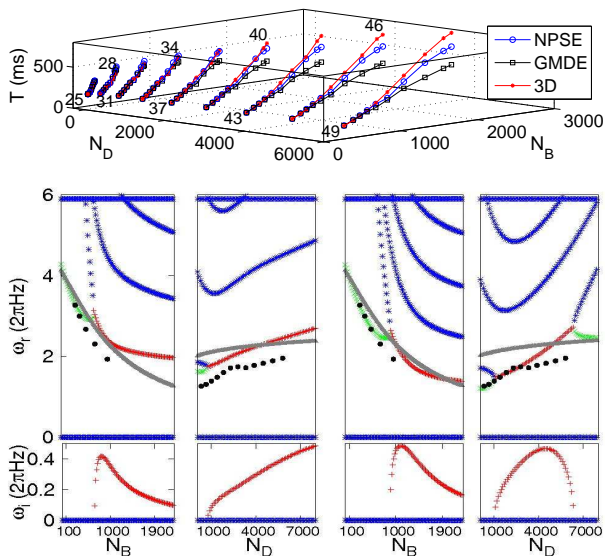


FIG. 2: (Color online) Top: DB soliton oscillation period vs.  $N_D$  and  $N_B$  for fixed  $\mu_D$  indicated by the numbers in the panel. Circles (blue) and squares (black) depict the results from the BdG analysis of the GMDE and NPSE, respectively; small (red) dots represent results of the 3D GPE. Bottom: BdG analysis of GMDE (left) and NPSE (right) [real  $\omega_r$  and imaginary  $\omega_i$  parts of the eigenfrequencies]: Anomalous mode (green), dynamically unstable mode (red), analytical 1D result of Ref. [10] (gray), and 3D GPE results (black points).

unstable, i.e., the amplitude of its oscillation increases. Such collisions are present in the DB soliton spectrum, and denote a critical difference in comparison with the case of dark solitons in single-species BECs. Furthermore, as observed in the right-most panel of Fig. 2 and also corroborated by our 3D GPE simulations, this oscillatory instability disappears for sufficiently large  $N_D$ .

From Fig. 2, we infer that for progressively larger atomic populations, a departure from the quasi-1D behavior emerges and a larger (smaller) oscillation frequency is obtained, if  $N_D$  ( $N_B$ ) is increased.

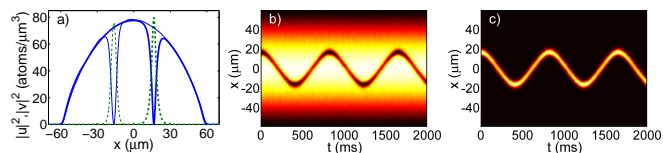


FIG. 3: (Color online) An oscillating DB soliton with period  $T = 827$  ms in the 3D GPE approach. Left panel: Transversal ( $y = z = 0$ ) cut of the density at  $t = 0$  (thick lines) and  $t = T/2$  (thin lines). Solid (dashed) line depicts the density for the dark (bright) component. Middle/right panels: Contour plots showing the evolution of the  $(y, z)$ -integrated density of the dark and bright solitons.

According to Fig. 2, the atom numbers used in Ref. [12] (up to  $N_B \sim 8000$  and  $N_D \sim 92000$ ) are out of the realm of validity of the effective 1D equations; thus, in this case, the 3D GPE has to be applied. Figure 3 illustrates

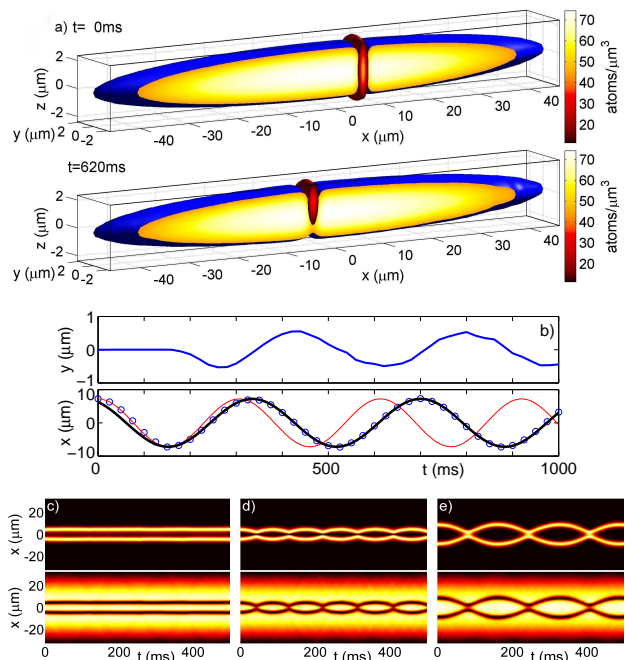


FIG. 4: (Color online) (a) Transverse oscillations of the DB soliton for  $(N_D, N_B) = (88\,181, 1\,058)$ . Top subpanel: initial condition. Bottom subpanel: a snapshot of the oscillating DB soliton at  $t = 620$  ms. (b) Transverse (top) and longitudinal (bottom) oscillations for the bright soliton. The thin (red) and thick (black) solid lines are sinusoidal fits to the longitudinal oscillations (circles) yielding periods  $T = 306$  ms (for  $t < 200$  ms) and  $T = 365$  ms (for  $t > 200$  ms), respectively. Bottom row of panels: Interaction of *two* DB solitons [top (bottom) subpanels depicting the bright (dark) component]. (c) In-phase (i.e. repulsive among bright) solitons close to their equilibrium position. (d) Out-of-phase (i.e. attractive among bright) solitons starting at the same location as in panel c). (e) Multiple collisions of in-phase solitons.

the oscillating DB soliton for trap frequencies and atom numbers comparable to those used in Ref. [12]. This 3D simulation results in an oscillating DB period of about 827 ms that is comparable with the period observed in Ref. [12] (slightly larger than 1 s). Possible sources for the discrepancy between the numerical and experimental oscillation periods include (i) high sensitivity of the period on the  $N_D$  to  $N_B$  ratio, (ii) sensitivity of the dynamics to uncertainties in the measured scattering lengths, and, perhaps more importantly, (iii) our numerics confirm that the oscillations are not harmonic and tend to have increasing periods for higher oscillating amplitudes.

The departure from the effective 1D description can be noticed, e.g., in panels (a) and (b) of Fig. 4. It is clear both from the oscillation snapshots (Fig. 4(a)) and from the evolution of the bright soliton center in the transverse direction (Fig. 4(b) top panel), that the DB soliton starts exploiting the transverse degrees of freedom shortly after release. Up to  $t < 200$  ms the soliton is at rest with respect to the transverse direction. For  $t > 200$  ms an os-

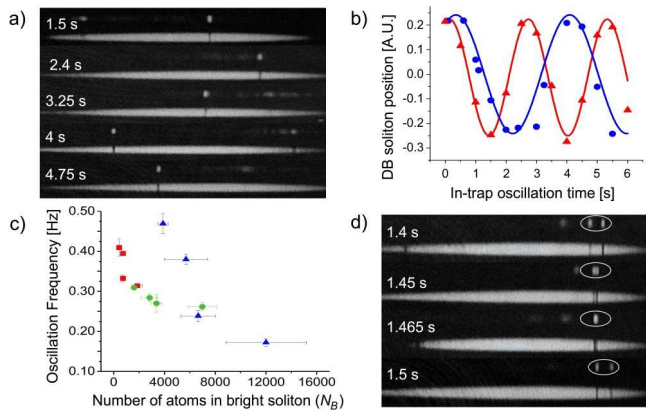


FIG. 5: (Color online) (a) Experimental images showing the oscillation of the DB soliton at the in-trap evolution times indicated. (b) In-trap DB soliton oscillation. Triangles (red) and squares (blue) correspond to, respectively,  $(N_B, N_D) \approx (680, 27\,000)$  and  $(N_B, N_D) \approx (9\,000, 650\,000)$ . Solid lines correspond to fitted harmonic oscillations with frequencies 0.39 Hz and 0.27 Hz respectively. (c) Oscillation frequency vs.  $N_B$  for different number of atoms in the dark component: squares (red):  $N_D \approx 30\,000$ , triangles (green):  $N_D \approx 200\,000$ , and circles (blue):  $N_D \approx 430\,000$ . (d) Experimental expansion images showing the oscillation and collision (in circled regions) of two DB solitons. Images in (a) and (d) are taken after 7 ms and 8 ms of free expansion for the bright and dark component, respectively. The components are vertically overlapped prior to expansion.

illation of the soliton occurs in the transversal direction leading at the same time to a reduction of the oscillation frequency in the axial direction (cf. thick (black) solid line in the bottom panel of Fig. 4b).

We also showcase 3D GPE simulations, cf. bottom row of panels in Fig. 4, depicting the interaction between *two* DB solitons [14]. Panel (c) shows a stationary DB pair with *in-phase*, i.e. mutually repulsive, bright soliton components (also, the dark ones always repel) that is balanced by the pull of the harmonic trap. Panel (d) depicts the evolution of the same initial DB pair as in panel (c), but with *out-of-phase*, i.e. mutually attractive, bright solitons, which yields an oscillatory dynamics. Panel (e) depicts the oscillations and collisions for in-phase bright solitons that were released at larger distances from the trap center and thus cannot avoid colliding despite their mutual repulsion. It is noteworthy that the DB collisions are apparently nearly elastic as the DB solitons retain their shape even after multiple collisions.

Finally, we present experimental data corroborating some principal points of our analysis (Fig. 5). Nonlinear effects in the counterflow of two BEC components are exploited to generate individual DB solitons [20]. The dark and bright component are formed by  $^{87}\text{Rb}$  atoms in the  $|1, -1\rangle$  and  $|2, -2\rangle$  state, respectively, for which  $a_{11} = 100.4 a_0$ ,  $a_{22} = 98.98 a_0$ , and  $a_{12} = 98.98 a_0$  [21]. The atoms are held in an elongated optical dipole trap with trapping frequencies  $\omega_{x,y,z} = 2\pi \times \{1.3, 163, 116\}$  Hz.

While the lack of exact cylindrical symmetry as well as the large atom number in the experiment preclude a direct comparison with our analytic results, the experiment clearly shows the anticipated decrease of oscillation frequency with increasing number of atoms in the bright and decreasing number of atoms in the dark component. Experimental results of the collision between two DB solitons are presented in Fig. 5(d), confirming their near-elastic nature.

*Conclusions.* We characterized the effectively 1D dynamics of DB solitons and showcased their potential dynamical instability. We demonstrated experimentally and theoretically the tunability of the oscillation frequency of a DB soliton. A spontaneous breaking of the cylindrical symmetry resulting in a reduction of the DB oscillation frequency was predicted, along with (also observed) near-elastic collisions, as well as a strong phase dependence of the collisional dynamics of DB solitons. Future directions include a detailed effective particle-based understanding of the DB soliton interactions, as well as a generalization of this picture towards the precession and interactions of vortex-bright solitons.

- 
- [1] P.G. Kevrekidis, D.J. Frantzeskakis, and R. Carretero-González, *Emergent Nonlinear Phenomena in Bose-Einstein Condensates*, Springer-Verlag (Berlin, 2008).
  - [2] Yu.S. Kivshar and G.P. Agrawal, *Optical solitons: from fibers to photonic crystals*, Academic Press (San Diego, 2003).
  - [3] M.J. Ablowitz, B. Prinari, and A.D. Trubatch, *Discrete and Continuous Nonlinear Schrödinger Systems*, Cambridge University Press (Cambridge, 2004).
  - [4] D.J. Frantzeskakis, *J. Phys. A* **43**, 213001 (2010).
  - [5] Z. Chen *et al.*, *Opt. Lett.* **21**, 1821 (1996).
  - [6] E.A. Ostrovskaya *et al.*, *Opt. Lett.* **24**, 327 (1999).
  - [7] C.J. Myatt *et al.*, *Phys. Rev. Lett.* **78**, 586 (1997).
  - [8] D.S. Hall *et al.*, *Phys. Rev. Lett.* **81**, 1539 (1998).
  - [9] D.M. Stamper-Kurn *et al.*, *Phys. Rev. Lett.* **80**, 2027 (1998).
  - [10] Th. Busch and J.R. Anglin, *Phys. Rev. Lett.* **87**, 010401 (2001).
  - [11] H.E. Nistazakis *et al.*, *Phys. Rev. A* **77**, 033612 (2008).
  - [12] C. Becker *et al.*, *Nature Phys.* **4**, 496 (2008).
  - [13] S. Rajendran *et al.*, *J. Phys. B* **42**, 145307 (2009).
  - [14] C. Yin *et al.*, arXiv:1003.4617.
  - [15] K.J.H. Law *et al.*, arXiv:1001.4835.
  - [16] L. Salasnich *et al.*, *Phys. Rev. A* **66**, 043603 (2002).
  - [17] F. Gerbier, *Europhys. Lett.* **66**, 771 (2004); A. Muñoz Mateo and V. Delgado, *Phys. Rev. A* **77**, 013617 (2008).
  - [18] G. Theocharis *et al.*, arXiv:0909.2122; A. Weller *et al.*, *Phys. Rev. Lett.* **101**, 130401 (2008); G. Theocharis *et al.*, *Phys. Rev. A* **76**, 045601 (2007).
  - [19] L. Salasnich and B.A. Malomed, *Phys. Rev. A* **74**, 053610 (2006).
  - [20] C. Hamner *et al.*, arXiv:1005.2610.
  - [21] Private communication by S. Kokkelmans.